Using pressure to probe thermodynamic anomalies in tetrahedrally-bonded materials

Jihui Nie[1,2], Sylwester Porowski[2] and Pawel Keblinski[1,2]

[1]Materials Science and Engineering Department, Rensselaer Polytechnic Institute, Troy, NY, USA

[2]Institute of High Pressure Physics, Polish Academy of Sciences, Warsaw, Poland

Tetrahedrally-bonded materials such as silicon, diamond, or gallium nitride, are characterized by low coordination number of 4 in the crystalline phase, and in general can exhibit a liquid phase with higher density and coordination. This leads to interesting thermodynamic behavior, including the lowering of the melting temperature with increasing pressure and the possible existence of distinct low- and high-density liquid phases. Using molecular dynamics simulations, we explored the role of pressure and the degree of tetrahedrality on the structure of and phase equilibria between the crystalline and liquid phases of tetrahedrally-bonded materials. In addition to the thermodynamic melting point, we determined the temperature of mechanical stability (spinodal temperature) as function of pressure. The latter temperature is relevant to the laser pulse rapid melting of tetrahedrally-bonded materials. The results of our simulations indicate the possibility of the existence of a thermodynamically stable low-density liquid phase of silicon at high pressures. Our simulation also suggests that GaN is unlikely to exhibit anomalous thermodynamic behavior due to a high degree of tetragonality preventing the formation of high-density liquid, even at high pressures.

1. Introduction and Motivation

Diamond-like semiconductors including those belonging to group IV, $A^{III}B^{V}$, and $A^{II}B^{VI}$, as well as other tetrahedrally coordinated materials (TCM) such as H_2O, due to their open, network structures, are characterized by a range of thermodynamic anomalies. One notable anomaly is that their density in the molten state is higher than it is in the crystalline phase as opposed to the typical situation in which the solid phase is denser than the liquid phase. As a consequence, for TCM, increasing pressure reduces the melting temperature.

The explanation of such behavior led to formulation of the now "classical" theory of these anomalies, known as Electronegativity Theory in Covalent Systems, and developed by Van Vechten in 1973.[1] This theory predicts that for all tetrahedrally bonded semiconductors, melting is accompanied by the drastic rearrangement of bonding, leading to the increase of the coordination number (CN) and consequently, to the increase of density upon melting.

Further progress in the understanding of those anomalies came from the advancement of molecular dynamics (MD) and associated empirical potentials capable of describing different bonding states of TCM. Most prominently, the first successful interatomic interaction potential for Si was developed by Stillinger and Weber in 1985.[2] The Stillinger-Weber (SW) potential (V_{SW}) was constructed from two short-range terms: a pairwise potential $V_2(r)$ and a three-body term $V_3(r, \theta)$, with $V_{SW} = V_2 + \lambda V_3$ (see Sect 2 for details). The V_3 term penalizes configurations with angles that are not tetrahedral, while V_2 drives the structure towards higher coordination. The competition between the two terms can be tuned by the selection of the scaling parameter λ, controlling the magnitude of the V_3 term relative to the magnitude of the V_2 term.

By a suitable selection of the λ parameter, one can model the basic structural and thermodynamic behavior of covalently bonded materials, such as Si, Ge, or C, and also water (H_2O),[3]. In the case of water, H_2O molecules can be represented by "atoms" (Monoatomic Water Model). This coarse-grained model without the explicit representation of hydrogen bonds or long-range electrostatic interaction is capable of reproducing the structure and phase diagrams of water.

Molinero et al[3] found that with increasing magnitude of the V_3 term (achieved by the increase of the tetrahedrality factor λ), the negative value of the volume change upon melting, ΔV, observed for a λ lower than 24, changes its sign and ΔV becomes positive for higher λ values. Consequently, materials with $\lambda > 24$ are expected to exhibit normal behavior, with the melting temperature increasing with pressure, while those $\lambda < 24$ are expected to exhibit opposite ("anomalous") behavior. This prediction is however limited to pressures near the ambient pressure, as the competition between the lower density covalently bonded structure and higher coordination structures can be altered at high pressures.

In this context, there is an ongoing discussion in the literature about the issue of gallium nitride (GaN). Utsumi et al.[4] observed that at pressures lower than 6 GPa GaN decomposes prior to melting, in agreement with previous data,[5] whereas at a pressure higher than 6 GPa, GaN melts with the melting temperature T_m more or less independent of pressure. Such behavior can be predicted by the SW potential with a suitable choice of λ mimicking GaN (also see section 3).

By contrast to purely covalent models of GaN such as the SW model, Harafuji et al.[6] proposed a MD model taking into account strong ionicity of GaN bonds and based only on

two body potentials, i.e. not explicitly representing the covalency of the bonds. This model predicts that short-range order remains largely unchanged upon melting, the coordination number (CN) in the liquid GaN is even smaller than 4, and the liquid volume is about ~20% larger than that of the crystal. Consequently, this model predicts a relatively steep increase of the GaN melting temperature with pressure. While this result is in disagreement with previously mentioned Utsumi et al. experimental data, it agrees with more recently published data.[7,8]

Motivated by the rich thermodynamic behavior of tetrahedrally-bonded materials, in this work using SW potentials and MD simulations, we will explore the impact of tetrahedrality strength and pressure on the equilibrium between solid and liquid phase and discuss possible consequences for real tetrahedrally-bonded materials. We note that recently results of extensive MD simulation studies on the effect of tetrahedrality on various water-like anomalies have been published.[9] In this context, our work zooms in on pressure effects on the liquid-solid coexistence and associated practical consequences. The next section will describe simulation methods and model systems. The results will be presented in Sec. 3, and we will conclude with a summary and discussion.

2. Models and Simulation Methods

The Stillinger-Weber (SW) potential[2] was extensively used to model tetrahedrally-bonded materials. It utilizes pairwise V_2 and three-body interaction V_3 to stabilize the diamond lattice crystal structure:

$$V = \sum_{i<j} V_2(i,j) + \lambda \sum_{i<j<k} V_3(i,j,k) \qquad (2.1)$$

where the magnitude of the dimensionless parameter λ characterizes the penalty for the deviation from the tetrahedral bonding geometry. Thus λ is often referred as the tetrahedrality

parameter. The SW potential was widely used in the studies on the anomalies in tetrahedral liquids.[10,11,12] Most prominently, the SW potential with λ = 21 extensively used to model silicon, was demonstrated to accurately reproduce density,[13] melting temperature,[14] elastic properties,[15] and phonon dispersion curves.[14]

In this work, in Eq. 2.1, except for λ we will use the parameter set of the original SW silicon potential.[2] We will treat λ as an adjustable parameter that we will vary from 20 to 26 which allows us to explore qualitatively the tetrahedrally-bonded materials with different degrees of tetrahedrality, as has been done in a number of previous MD studies.[9,12] All MD simulations were performed using the LAMMPS package[16] with a time step of 1 fs.

The thermodynamic melting temperature (T_m) was determined through the phase coexistence method involving planar liquid-solid interfaces following the protocols of Ref. [17]. In brief, we first melt ½ of the crystal in the simulation cell with dimension $40\ \text{Å} \times 40\ \text{Å} \times 160\ \text{Å}$, containing 16384 atoms in each case as illustrated in Fig. 1 (top panel). In particular, we initially keep the atomic positions fixed in the intended crystalline part (central region in Fig 1), while melting the other part at high temperature of 2500 K, allowing the thermal expansion (or contraction) of the simulation cell to accommodate the volume change associated with melting. In the next step, we lower the temperature of the liquid to the vicinity of the expected thermodynamic melting point (e.g., to 1700 K in the case of λ = 21), and finally we allow the whole system to evolve without any constraints at constant pressure and enthalpy conditions for 100 ps. During the final step of the simulations, the temperature of the system evolves, either due to melting or crystallization, towards T_m and finally fluctuates in equilibrium around the thermodynamic melting temperature. For selected cases, we increased the cross section by a factor of 4 and observed that within the statistical errors

the melting point is the same, indicating the negligible size effect on the thermodynamic melting temperature determination.

Once the system reaches equilibrium, in addition to T_m, we determine other structural characteristics in both liquid and crystal regions by dividing the system into 5.43 Å wide slabs, evaluating characteristics of each slab and performing time averages. For example, in the bottom panel of Fig. 1, we show profiles of average atomic coordination for equilibrium structures of coexisting crystal and liquid for λ = 21 (SW silicon model) and λ = 26 (SW model representative of carbon) obtained in this way. As expected, in both cases the crystalline case has an average coordination = 4 as the characteristics of perfect tetrahedral bonding. However, the λ = 21 case exhibits an average coordination in the liquid of 5.3 due to the significant reduction of the tetragonal bonding character towards higher coordinated metallic bonding. In the case of λ = 26, the liquid average coordination is 4.4, i.e. in this case the liquid exhibits a much larger degree of tetragonality.

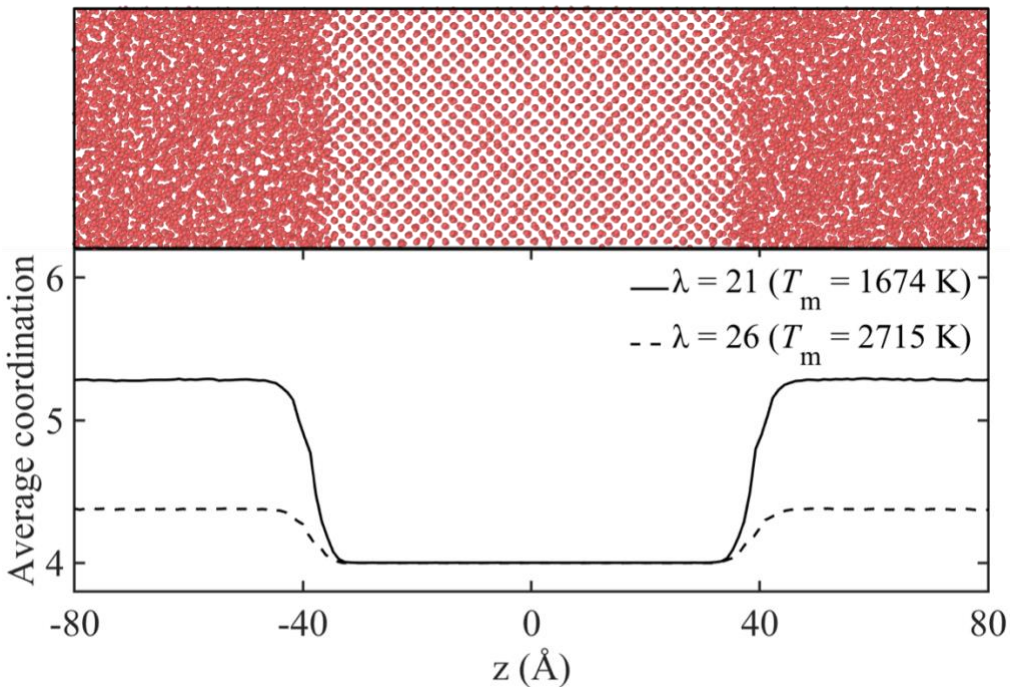

Figure 1. The typical atomic configuration of an equilibrated SW system with coexisting liquid and crystal phases (top panel) and the corresponding average coordination profiles (bottom panel) for SW systems with $\lambda = 21$ and $\lambda = 26$ at 0 GPa and their thermodynamic melting temperatures (T_m).

When the simulation cell contains just perfect crystal, upon temperature increase, the structure does not melt at the thermodynamic melting point due to the nucleation barrier. Consequently, one has to reach the spinodal temperature, at which the nucleation barrier disappears— for crystal at this temperature, some elastic constants are reduced to zero.[18] Therefore, the spinodal temperature in this case can be also called the mechanical instability point (T_s). Such temperature is of interest for comparative purposes with T_m but is also relevant to laser pulse-melting experiments[19, 20] where picosecond heating bypasses the nucleation process and the structure melts, or rather collapses to melt, at or near T_s.

We determine the mechanical instability point T_s from the collapse of perfect crystal in the following manner. We use a perfect crystal structure in the cubic simulation cell with 4096 atoms and heat it at constant pressure from 1500 K to 4000 K at a rate of 1 K/ps. Concurrently, we monitor various quantities, such as density, bonding (potential) energy, and the average coordination, to detect structural changes. All these quantities exhibit sharp changes during the phase change, as illustrated by the average coordination data in Fig. 2. The intersection point of two linear fitting curves of the pure crystal region and the crystal-liquid mixture region is evaluated as the mechanical instability point of the SW system as shown in Fig. 2.

As shown in Fig. 2, the phase change is very rapid with about 10 ps needed to create a large pocket of liquid (see atomic snapshot in the bottom right corner of Fig. 2) and additional 10 ps for a complete transformation to the liquid structure. In the plot of the average coordination vs. temperature (or equivalently vs. time as the heating rate is constant), we use two linear portions of the curve to determine (and operationally define) T_s by the intersection of the two fitting lines (see Fig.2). We note that according to Fig. 2 at the incipient of the phase change, a nucleus of the liquid phase appears. This suggests that we only approach spinodal decomposition temperature (mechanical instability temperature) and we actually observe a nucleation process. Consequently, one can expect that such determined instability temperature is dependent on the heating rate and the system size. Further discussion is provided in the last part of next section (see Fig. 8).

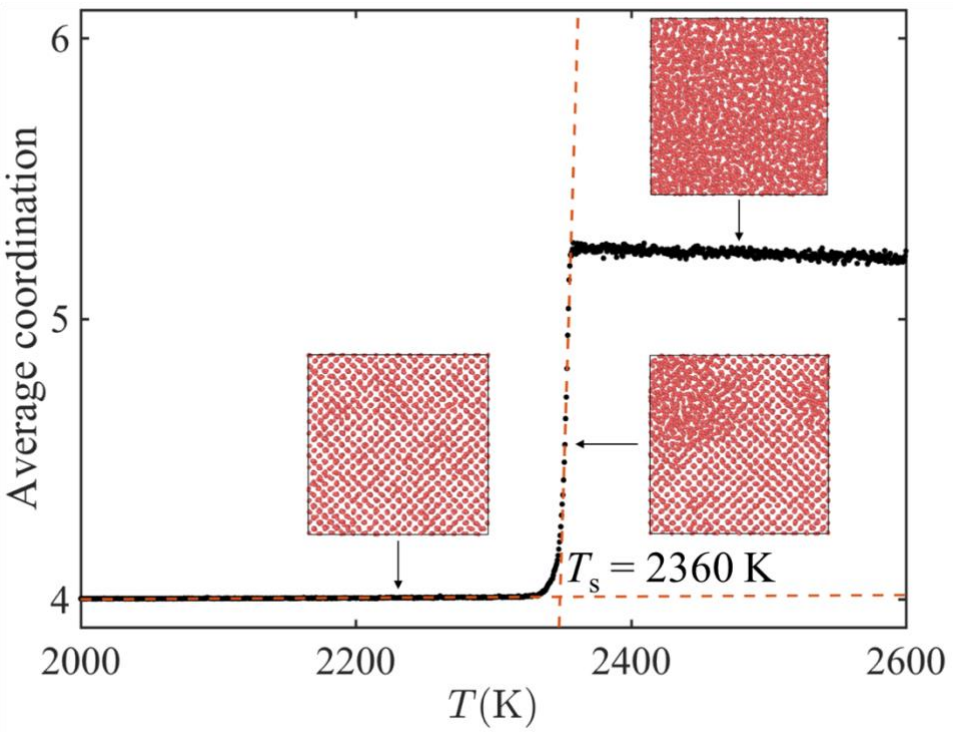

Figure 2. The variation of average coordination of the SW perfect crystal system with λ = 21 at 0 GPa when the temperature increases. Two dash lines are linear fitting curves for the crystal region and the crystal-liquid mixture region respectively. The intersection point of two fitting curves is used to evaluate the mechanical instability point (T_s).

We also use the same cubic simulation cell to determine other properties in single phases, including atomic volume, bulk modulus, and average coordination as a function of pressure and temperature. In these cases, the single phase (crystal or liquid) systems were equilibrated at target pressures and corresponding thermodynamic melting temperatures under the NPT ensemble for 1 ns, and we collected the data averaged during the last 600 ps. The bulk modulus B is defined as

$$B = -V\frac{dP}{dV} \tag{2.2}$$

where V is the system volume and P is the pressure. We monitored the equilibrium volume of the single phase at each pressure and the corresponding melting temperature, and obtained the bulk modulus from the slope of the P-ln(V) curve (not shown). The coordination number is the average number of nearest neighbors. The nearest neighbors are defined as atomic pairs within the distance smaller than the position of minimum in the radial distribution function between the first and second peak.

3. Results

Using the simulation of coexisting liquid and crystal phases (see Fig. 1), we determined T_m as a function of pressure for λ ranging from 20 to 26 and pressures up to 20 GPa. The results are presented in Fig. 3. In all cases, we also explored negative pressures, typically up to 2 or 3 GPa. At lower negative pressure, the structures become unstable due to cavity formation.

Consistent with the literature data,[3,9] the first observation is that for λ ranging from 20 to 23
in the whole pressure range studied, T_m decreases with increasing pressure. This behavior is associated with the fact that contrary to most materials, tetrahedrally bonded materials often exhibit a liquid phase with a higher density than the crystal phase. Consequently, increasing

pressure stabilizes the liquid phase and in agreement with the prediction of the well-known thermodynamic Clausius–Clapeyron relation, the melting point decreases with increasing pressure. We also notice that we do not see any evidence of the T_m maximum in the case of silicon (λ = 21), while some suggested that such maximum exists at the negative pressure region.[21, 22] We see an incipient of such maximum at negative pressures for λ = 24. For λ = 25 there is a clear maximum, however, only at positive pressure. In both cases, the maximum is followed by the minimum and then the T_m increases with pressure again. In the case of λ = 26, the maximum and the minimum appear to merge, and at most, there is an inflection point present, with T_m monotonically increasing with pressure across the whole pressure range, thus representing no anomalous material behavior.

We note that for all values of λ parameters and pressure-temperature conditions studied in this work, we did not observe a solid-solid phase transition from a low coordination diamond crystal structure to higher coordinated solid structures, such as β-Sn structure. For example, in the case of Si, it is known that such transition occurs at P~ 11-12 GPa.[23] The existence of such a transition, of course, would affect the liquid-crystal equilibrium.

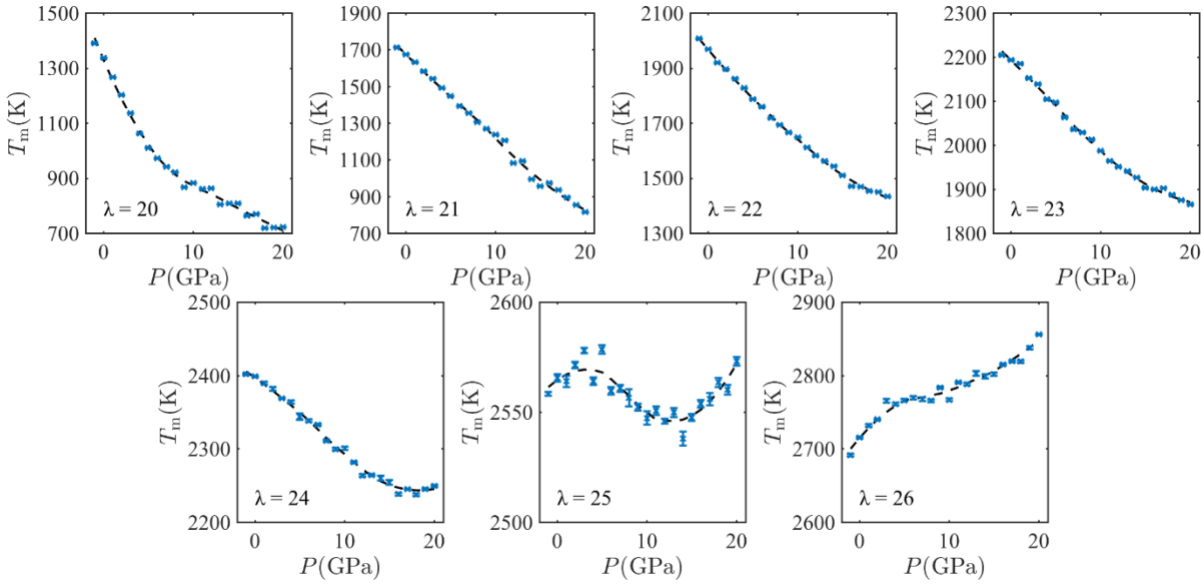

Figure 3. The thermodynamic melting temperatures of the SW systems as function of pressures for different values of the tetrahedral parameter.

To gain an understanding of the behavior presented in Fig. 3, we evaluated the atomic volume difference between liquid and crystal phases, ΔV, as a function of pressure at the corresponding melting temperature. In the range of $\lambda = 20$ to $\lambda = 23$, the difference is always negative, i.e., the liquid is denser than the crystal, and upon melting, the volume decreases. Consequently, according to the Clausius–Clapeyron relation, T_m is expected to decrease with increasing pressure, as indeed is the case (see Fig. 3). For $\lambda = 24$ and 25, ΔV changes sign twice—this corresponds to the maxima and minima in T_m vs P plots (see Fig. 3). Finally, for $\lambda = 26$, ΔV is always positive and consequently T_m monotonically increases as P increases.

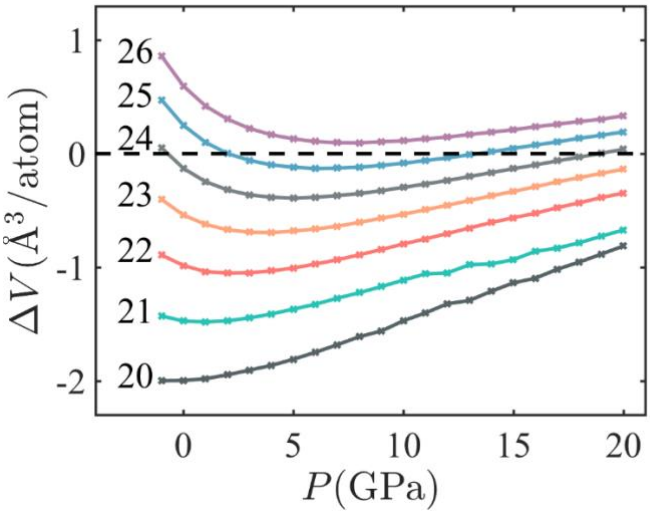

Figure 4. The volume difference between SW crystals and liquids as a function of pressure at the corresponding melting temperatures for λ ranging from 20 to 26.

It is interesting to note that for all λ values, ΔV as a function of pressure plots exhibit positive curvature and ΔV first decreases and later increases. To understand this behavior, we

evaluated the bulk modulus of the crystal and liquid phases as function of pressure at the corresponding T_m. The results are presented in Fig. 5. For all λ values studied at low pressures, liquid is softer than crystal, consequently at low pressures ΔV decreases with increasing pressure. However, as the pressure increases, the liquid stiffens at a much higher rate than the solid, and the liquid modulus becomes higher than the crystal modulus. At this point ΔV starts to increase with increasing pressure (see Figs 4 and 5).

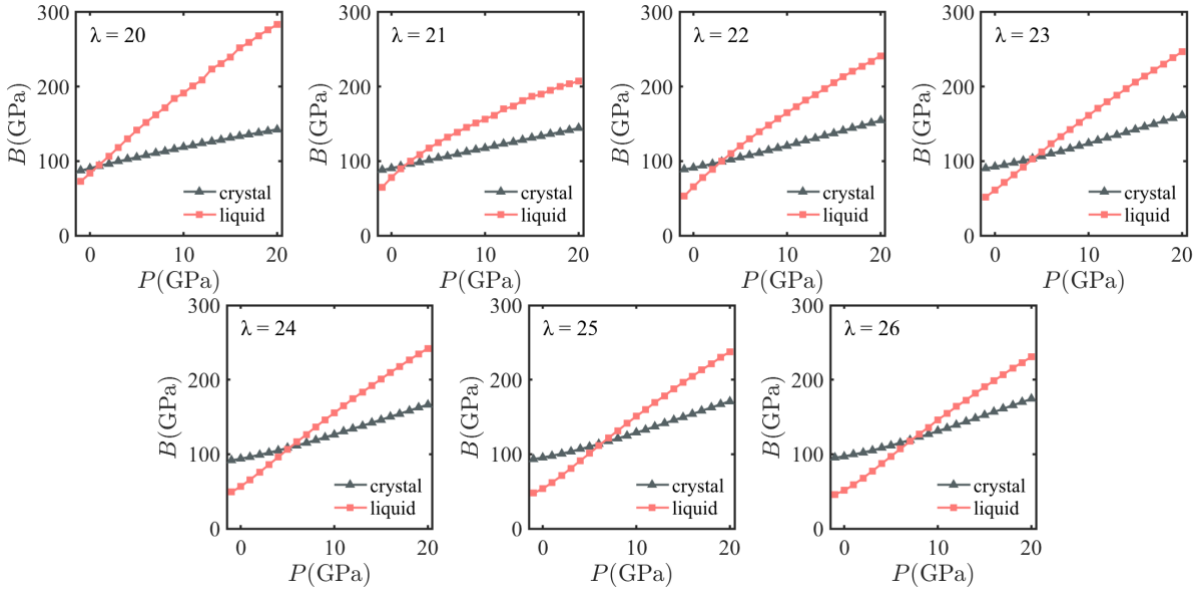

Figure 5. The bulk moduli of the SW crystals and liquids with different tetrahedral parameters λ as a function of pressure at the corresponding melting temperatures. The intersection points of two curves correlate with the minima locations in Fig. 4.

As we discussed above for the model of silicon (λ = 21), we did not observe any signature of high temperature maxima of the melting point at negative pressures. Such maxima, if it does exist, would suggest an existence of a less dense and more tetrahedrally-coordinated liquid and an associated liquid-liquid phase change.[24] While such low-density liquid formation was not observed by the pressure reductions, it is well known that in molecular dynamics

simulations SW liquids exhibit a transformation from high to low-density liquid upon temperature decrease.[24, 25]

To illustrate the above statement, Fig. 6 shows how the average coordination of SW liquids changes upon quenching at zero pressure from high to low temperatures. For all λ values, upon temperature decrease, the coordination increases as some bonds broken by high temperature agitation are reformed. However, in all cases the coordination reaches maximum and upon further temperature decrease, the coordination decreases. This decrease is associated with a transformation of the high coordinated liquid phase to low coordinated liquid phase. For higher values of λ at low temperatures, the coordination is very close to 4, characterizing a tetrahedrally bonded network. For lower λ the coordination is significantly higher than 4. However, this is mostly due to the kinetics of the fast quench rate. At lower quench rates, even for lower λ values, the coordination at a low temperature would be closer to 4.

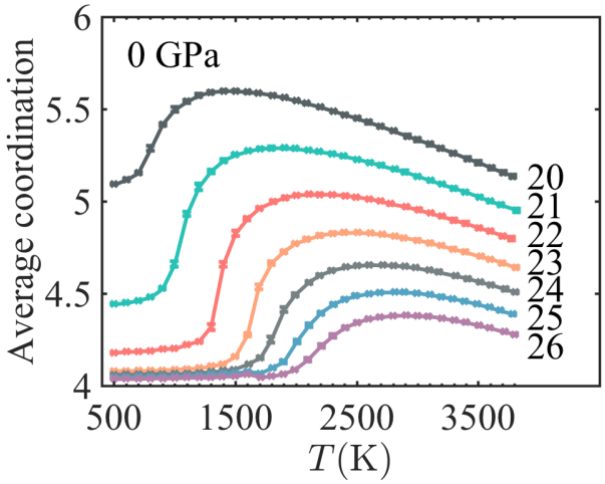

Figure 6. The average coordination of SW liquids at 0 GPa as a function of temperature obtained by the quenching of the liquid from 3800 K to 500 K at the rate of 1 K/ps.

While the liquid-liquid transition occurs in MD simulations at low temperatures, for the real materials quenched at much lower rates, instead of a transformation to a low-density liquid, one would observe crystallization. However, for low λ values, such as in the case of λ = 21 (silicon model), with increasing pressure the thermodynamic melting temperature decreases significantly. This creates an intriguing possibility that one can observe equilibrium liquid-liquid phase change induced by lowering of the temperature in the system with coexisting crystal and liquid upon application of pressure.

To test the above-discussed possibility, we monitored the average coordination in the coexisting liquid and crystal phases. The results presented in Fig. 7 show that indeed, for lower λ values, particularly λ = 21 (Si), the coordination of the liquid first increased with the increasing pressure, but later reached the maximum and decreases. This result suggests that the liquid-liquid phase change might be possible to observe for silicon in equilibrium upon the application of high pressure.

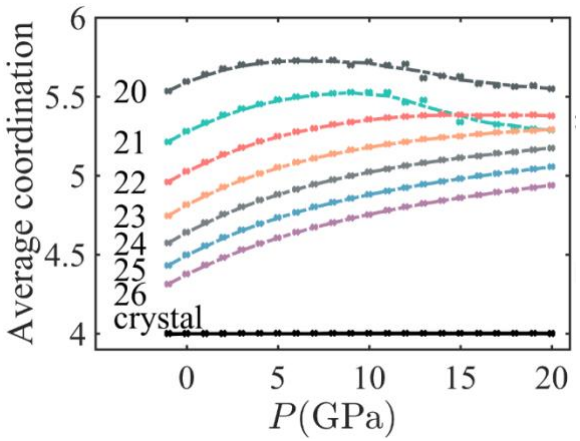

Figure 7. The average coordination the SW crystals and liquids as a function of pressure at the corresponding melting temperatures.

Finally, we examined how the mechanical instability temperature depends on pressure for a range of λ parameters. In this case we observed "instantaneous" melting of a crystal in a periodic simulation cell without any defects present (see Fig. 2). While such instability occurs well above the thermodynamic melting point, it is relevant to rapid melting by laser pulses. Despite the short time scale of the heating process, we observe the liquid phase nucleation (see Fig.2). The resulting dependence on the heating rate and the system size of the mechanical instability temperature is shown in Fig. 8. The mechanical instability temperature increases with increasing heating rate, which is associated with the hysteresis effect in the superheating process. As the system size increases, the mechanical instability temperature decreases because there are more possible sites for the nucleus formation in the larger volume. For the rest of the work, we use the heating rate of 1 K/ps to investigate the dependence of the mechanical instability temperature on the pressure.

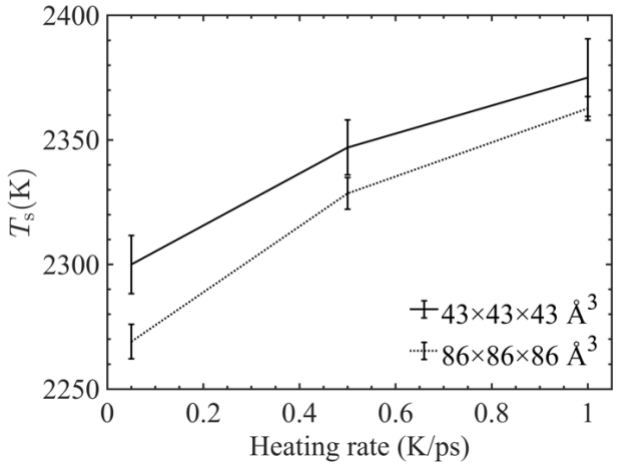

Figure 8. The system size and heating rate dependence of the mechanical instability temperature of SW perfect crystals with λ = 21.

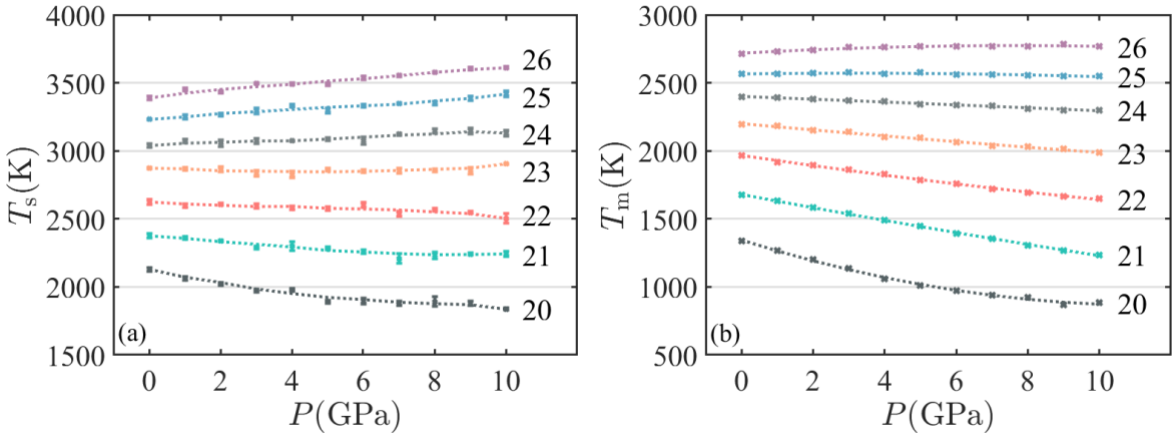

Figure 9. (a) The mechanical instability temperatures of SW perfect crystals as a function of pressures for several values of λ. (b) The thermodynamics melting point (data are the same as in Fig. 3) presented in a form allowing for a better direct comparison with the data presented in panel (a).

The value of the mechanical instability temperature as a function of pressure is presented in Fig. 9 (a). By comparison with the thermodynamic melting point pressure dependence (see Fig. 9 (b)), the mechanical instability temperature is consistently much larger (by about 500 K). For lower values of λ, increasing pressure leads to the decrease of the mechanical instability temperature, while the opposite is true for larger λ values. This behavior, in general, is similar to the pressure dependence of the thermodynamic melting point. However, the details are different. In particular, in the case of the mechanical instability temperature, the least pressure dependence is exhibited by λ =23 case, while in the case of the thermodynamic melting point, the least pressure dependence is exhibited by λ =25 case.

4. Summary and Discussion

We used MD simulations and SW empirical potentials to explore the influence of pressure and the degree of tetrahedrality on the structure and phase equilibria between crystalline and liquid phases of tetrahedrally-bonded materials. For a lower degree of tetrahedrality (such as that characterizing Si and Ge), we observed that upon melting, the structure densifies, even at negative pressures. Our results also indicate that silicon might exhibit an equilibrium transition from a higher to lower density liquid structure at the 10-15 GPa pressure range due to a rapidly decreasing melting point. This originates from the fact that despite of an increasing pressure that favors the high-density liquid phase, the effect of a rapidly decreasing melting temperature that favors a low-density liquid phase might dominate.

For a higher degree of tetrahedrality (such as that characterizing GaN), the SW potentials predict a limited effect of pressure on the melting temperature, which in the case of GaN is inconsistent with the behavior deduced from recent experimental data,[7,8] indicating a significant melting point increase with increasing pressure. This inconsistency might be due to the fact that the SW potential does not reflect an ionic nature of interatomic interactions, and thus might underestimate the volume change upon melting, as suggested by MD simulations of an ionic model of GaN[6]. From the modeling perspective, more accurate determination of the volume change of GaN upon melting will require first-principle based calculations which are unencumbered by the approximate nature of empirical interatomic potentials.

Interestingly, regardless of the degree of tetrahedrality represented by SW potentials, at high enough pressures we observed normal behavior with the melting point increasing upon pressure increase. This originates from the fact that the liquid phases stiffen with pressure at a

much faster rate that the crystal phases. This behavior might be universal for covalently bonded crystals, but it might also just characterize SW models. Again, first principle calculations are highly desired here to assess the universality of the above observation.

In addition to the thermodynamic melting point, we determined the temperature of mechanical stability (spinodal temperature) as function of pressure. The latter temperature is relevant to laser pulse rapid melting. The comparison between the thermodynamic melting point and the mechanical stability temperature suggest that the two processes are qualitatively related, but quantitative comparison reveals significant differences. This suggest that laser pulse rapid melting experiments have a limited ability to assess the thermodynamic behavior of covalently bonded materials. However, they may be relevant in studies of the structure of liquid phases which are otherwise difficult or not accessible to direct experimental observations.

Acknowledgment: The work of J.N. and P.K. was supported by the European Union's Horizon 2020 Research and Innovation Programme under the Marie Skłodowska-Curie Grant Agreement No. 665778 via the Polish National Science Centre Polonez program (No. 2016/23/P/ ST3/04290). We are also grateful for fruitful discussions with Professor Izabella Grzegory from the Institute of High Pressure Physics at the Polish Academy of Sciences.

References:

[1] J.A., Van Vechten, Physical Review B, **7**, 1479 (1973).

[2] F.H. Stillinger and T. Weber, Phys. Rev. B **31**, 5262 (1985).

[3] V. Molinero, and E.B. Moore. J. Chem. Phys. B, **113**, 4008 (2009).

[4] W. Utsumi et al., Nature Materials **2**, 735 (2003).

[5] J. Karpinski, J. Jun, and S. Porowski, Journal of Crystal Growth **66**, 1-10 (1984).

[6] K. Harafuji, T. Tsuchiya, and K. Kawamura. J. Appl. Phys. **96**, 2501 (2004)

[7] Porowski, S., et al., J. Phys. Chem. Sol. **85**, 138 (2015).

[8] Porowski, S., et al., J. Cryst. Growth, **505**, 5 (2019).

[9] J. Russo, K. Akahane, and H. Tanaka, PNSA **115**, E3333 (2019).

[10] D. Dhabal, C. Chakravarty, V. Molinero, and H.K. Kashyap, J. Chem. Phys. **145**, 214502 (2016).

[11] S. Sengupta, V.V. Vasisht, and S. Sastry, J. Chem. Phys. **140**, 044503 (2014).

[12] W. Hujo, B. Shadrack Jabes, V.K. Rana, C. Chakravarty, and V. Molinero, J Stat Phys **145**, 293 (2011).

[13] S.J. Cook and P. Clancy, Phys. Rev. B **47**, 7686 (1993).

[14] J.Q. Broughton and X. Li, Phys. Rev. B **35**, 9120 (1987).

[15] M. D. Kluge, J. R. Ray, and A. Rahman, J. Chem. Phys. **85**,4028 (1986).

[16] S. Plimpton, J. Comput. Phys. **117**, 1 (1995).

[17] P. Keblinski, M.Z. Bazant, R.K. Dash, and M.M. Treacy, Phys. Rev. B **66**, 1924 (2002).

[18] J Wang, J Li, S Yip, S Phillpot, D Wolf Physical Review B **52**, 12627 (1995).

[19] P.L. Liu, R. Yen, N. Bloembergen, and R.T. Hodgson, Appl. Phys. Lett. **34**, 864 (1979).

[20] J.M. Liu, R. Yen, H. Kurz, and N. Bloembergen, Appl. Phys. Lett. **39**, 755 (1981).

[21] P.F. McMillan, Nat Mater **1**, 19 (2002).

[22] M. Wilson and P.F. McMillan, Phys. Rev. Lett. **90**, 570 (2003).

[23] J.Z Hu, and L. Spain, Sol. Sta. Comm. 51, 263 (1984).

[24] J.N. Glosli and F.H. Ree, Phys. Rev. Lett. **82**, 4659 (1999).

[25] S. Sastry and C. Austen Angell, Nat Mater **2**, 739 (2003).